UC Irvine
UC Irvine Previously Published Works

Title

Are rotating planes of satellite galaxies ubiquitous?

Authors

Phillips, John I
Cooper, Michael C
Bullock, James S
et al.

Are rotating planes of satellite galaxies ubiquitous?

John I. Phillips[1]⋆, Michael C. Cooper[1]†, James S. Bullock[1],
Michael Boylan-Kolchin[2]

[1] *Center for Cosmology, Department of Physics and Astronomy, 4129 Reines Hall, University of California Irvine, CA 92697, USA*
[2] *Astronomy Department, University of Maryland, College Park, MD 20742-2421*

21 August 2015

ABSTRACT

We compare the dynamics of satellite galaxies in the Sloan Digital Sky Survey to simple models in order to test the hypothesis that a large fraction of satellites co-rotate in coherent planes. We confirm the previously-reported excess of co-rotating satellite pairs located near diametric opposition with respect to their host, but show that this signal is unlikely to be due to rotating discs (or planes) of satellites. In particular, no overabundance of co-rotating satellites pairs is observed within $\sim 20° - 50°$ of direct opposition, as would be expected for planar distributions inclined relative to the line-of-sight. Instead, the excess co-rotation for satellite pairs within $\sim 10°$ of opposition is consistent with random noise associated with undersampling of an underlying isotropic velocity distribution. Based upon the observed dynamics of the luminous satellite population, we conclude that at most 10% of isolated hosts harbor co-rotating satellite planes (as traced by bright satellites).

Key words: Local Group – galaxies: formation – galaxies: evolution – galaxies: dwarf – galaxies: star formation

1 INTRODUCTION

Within the ΛCDM paradigm, the growth of cosmic structure proceeds as overdensities collapse into dark matter halos, which eventually serve as the sites for galaxy formation (White & Rees 1978; Blumenthal et al. 1984; Davis et al. 1985). Over time, the hierarchical accretion and merging of halos drives the development of substructure, such that some halos reside within the bounds of larger parent halos (Moore et al. 1998). The galaxies hosted by these subhalos are typically referred to as satellites and are important probes of the evolution of substructure, as they serve as tracers of dark matter on small scales.

High-resolution *N*-Body and hydrodynamic simulations confirm this picture of hierarchical structure formation, while also making predictions regarding the properties of subhalos and the satellite galaxies they host. In particular, simulated subhalos are not isotropically distributed with respect to their parent dark matter halo. Instead, simulations across a broad range of mass scales predict that satellite galaxies should preferentially lie along orbits aligned with the major axis of the host halo (e.g. van den Bosch et al. 1999; Knebe et al. 2004; Libeskind et al. 2005; Kang et al.

2007; Lovell et al. 2011; Wang, Frenk & Cooper 2013). Two possible physical drivers are often associated with this predicted alignment of substructure with the shape of the larger gravitational potential: [*i*] preferential destruction (or suppression) of satellites on orbits anti-aligned with the halo's major axis (Zaritsky & Gonzalez 1999; Peñarrubia, Kroupa & Boily 2002; Pawlowski et al. 2012) or [*ii*] accretion of satellites along preferred directions, perhaps associated with large-scale filaments (Zentner et al. 2005; Libeskind et al. 2011).

Observations of galaxies in nearby groups and clusters largely support the predicted anisotropies found in simulations, such that satellites in massive dark matter halos are preferentially aligned with the major axis of the central galaxy and with the larger-scale, filamentary structure (e.g. West & Blakeslee 2000; Plionis et al. 2003; Faltenbacher et al. 2007; Hao et al. 2011; Tempel et al. 2015). When pushing to lower-mass, more-isolated halos, studies based on large spectroscopic samples similarly find that satellites preferentially reside along the major axis of red (or early-type) hosts, while the distribution of satellites around blue (or late-type) hosts is consistent with being isotropic (Brainerd 2005; Sales & Lambas 2004, 2009; Yang et al. 2006; Azzaro et al. 2007; Bailin et al. 2008, but see also Zaritsky et al. 1997). This apparent lack of spatial anisotropy for satellites of late-type hosts is potentially driven by random misalign-

⋆ e-mail: johnip@uci.edu
† e-mail: cooper@uci.edu

ment between the major axis of the host's disc and the dark matter halo, such that the satellites may be aligned with the latter but not the former (Bailin et al. 2005; Libeskind et al. 2007; Deason et al. 2011).

In contrast to the satellites of comparable star-forming hosts in the local Universe, observations of the Local Group suggest that the spatial distribution of satellites around both the Milky Way and M31 are significantly anisotropic. In particular, the satellites of the Milky Way preferentially reside near the northern and southern Galactic poles (i.e. along the minor axis of the Milky Way disc, Holmberg 1969), possibly following a planar arrangement (Lynden-Bell 1976; Kunkel & Demers 1976; Metz, Kroupa & Jerjen 2007; Pawlowski, Pflamm-Altenburg & Kroupa 2012). The satellites of M31 are similarly anisotropic in their distribution, with a large subset belonging to a thin disc or plane (Karachentsev 1996; Koch & Grebel 2006; McConnachie & Irwin 2006; Metz, Kroupa & Jerjen 2009; Conn et al. 2013).

When including velocity information, the anisotropy of the Local Group satellite distribution becomes even more pronounced, with many of the Milky Way satellites following polar obits, consistent with a vast, coherently-rotating plane (Metz, Kroupa & Libeskind 2008; Pawlowski, Kroupa & Jerjen 2013; Pawlowski & Kroupa 2013). For M31, a yet more-striking planar structure is observed, such that a large number of satellites exhibit coherent rotation along the line-of-sight to the Milky Way, forming a vast plane with a diameter of ~ 400 kpc and a thickness of less than ~ 15 kpc (Ibata et al. 2013). While simulations predict that satellites should preferentially align with the major axis of the host dark matter halo, the strong anisotropies observed for the Local Group satellites (especially those around M31) are inconsistent with the expectations of simulated subhalo populations (Kroupa, Theis & Boily 2005; Kroupa et al. 2010; Pawlowski et al. 2012, 2014; Ibata et al. 2014c, but see also Buck, Macci'o & Dutton 2015, who argue that co-rotating planar arrangements of satellites are predicted by ΛCDM).

The striking nature of the M31 satellite disc has served as fuel for many recent studies investigating the possibility of similar, strongly-anisotropic satellite distributions around galaxies outside of the Local Group, such as the discovery of possible planar structure in the satellite distribution of the Centaurus A group (Tully et al. 2015; Libeskind et al. 2015). In particular, recent analysis of satellite pairs in the Sloan Digital Sky Survey (SDSS, York et al. 2000) points towards the possibility of co-rotating planar satellite structures around nearby massive galaxies (Ibata et al. 2014a, hereafter I14); for 20 out of 22 systems, with satellite pairs located on diametrically-opposed sides of the host galaxy, I14 detect co-rotation along the line-of-sight, suggesting that thin satellite planes – similar to that of M31 – may be relatively common. Specifically, this result, which is supported by an analysis of the spatial positions of photometrically-selected satellite samples, indicates that $\gtrsim 50\%$ of the satellite population may reside in thin co-rotating planes (Ibata et al. 2014b, although Cautun et al. 2015 argue that the evidence for the ubiquity of such planar structures is not robust). Given the scarcity of such structures in modern simulations (Ibata et al. 2014c; Pawlowski & McGaugh 2014, see Cautun et al. 2015 for an argument that the diversity of properties of these structures accounts for their perceived
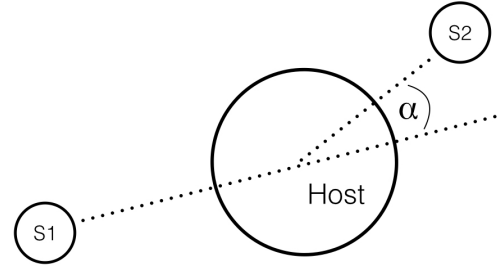

Figure 1. Definition of the opening angle (α) between satellite pairs (here, S1 and S2), as measured with respect to the host galaxy. Each satellite pair has a uniquely defined α, ranging from $0°$ to $180°$, such that satellites on diametrically-opposed sides of a host correspond to $\alpha = 0°$.

rarity.), the analysis of I14 poses a strong test of the ΛCDM cosmology and thereby warrants further investigation.

In this paper, we re-examine the kinematic evidence for the existence of co-rotating planes of satellites around nearby massive hosts by comparing the coherence of line-of-sight velocities of observed satellite galaxies to simple models of satellite spatial distributions and kinematics. The structure of the paper is as follows: in §2, we discuss the selection of the observational sample and the measured abundance of co-rotating satellite pairs. In §3, we introduce our numerical models and compare the mock observations derived from the models to the observational data. Finally, in §4, we discuss our results in the context of the search for M31-like planes elsewhere in the Universe. Throughout our analysis, we employ a Λ cold dark matter (ΛCDM) cosmology with WMAP7+BAO+H_0 parameters $\Omega_\Lambda = 0.73$, $\Omega_m = 0.27$, and $h = 0.70$ (Komatsu et al. 2011), and unless otherwise noted all logarithms are base 10. Throughout the paper, we use the terms "[satellite] disc" and "[satellite] plane" interchangeably, referring to co-rotating planar satellite configurations.

2   OBSERVATIONAL DATA

2.1   Sample Selection

We draw our observational data from Data Release 7 (DR7, Abazajian et al. 2009) of the SDSS, making use of the derived data products from the NYU Value-Added Galaxy Catalog (VAGC, Blanton et al. 2005) including absolute r-band magnitudes (M_r) that are K-corrected to $z = 0.1$ using KCORRECT (Blanton & Roweis 2007). Throughout this work, we restrict our analysis to regions of the SDSS where the spectroscopic completeness exceeds 70% (i.e. FGOT-MAIN > 0.7). We also reject all galaxies with line-of-sight velocity errors greater than 25 km/s.

In selecting our galaxy sample, we adhere closely to the procedure of I14. We select a sample of hosts in the magnitude range $-23 < M_r < -20$ and within a redshift
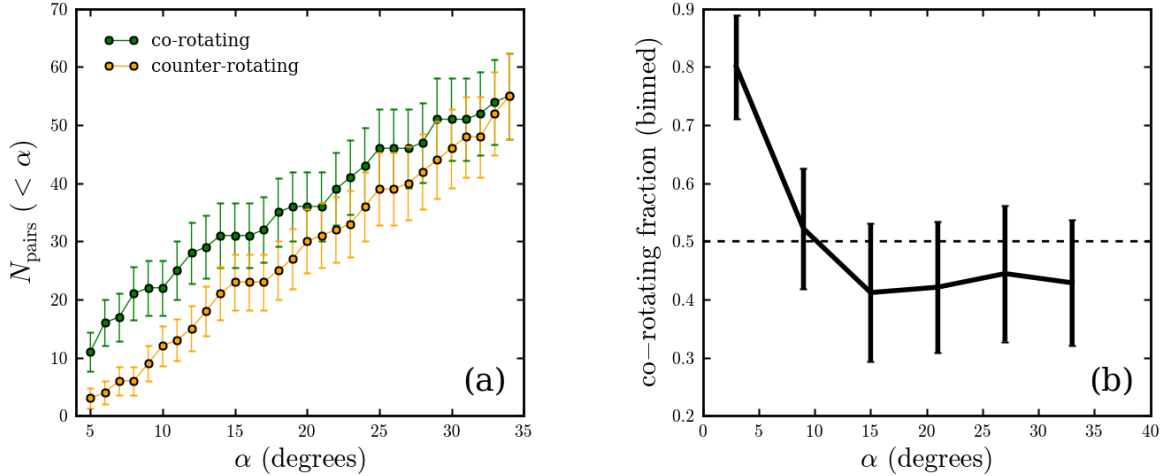
Figure 2. *Left*: the cumulative number of co-rotating (green line) and counter-rotating (orange line) satellite pairs as a function of opening angle (α), including uncertainties based on Poisson statistics. *Right*: the fraction of co-rotating satellite pairs as a function of opening angle, computed in distinct bins of α (bins have width $6°$), with error bars derived according to the binomial theorem. There is a significant excess of co-rotating satellite pairs over counter-rotating pairs at small α (i.e. for satellites that are nearly diametrically opposed to each other). This overabundance of co-rotating pairs suggests the possible presence of coherently-rotating planar satellite structures around nearby massive host galaxies (however, see Fig. 3).

range of $0.002 < z < 0.05$. A host is considered isolated if there are no brighter objects within 500 kpc (in projection) on the sky and within 1500 km/s in velocity space. Only isolated systems are retained, reducing the number of hosts to $22,780$ isolated galaxies. From this set of host systems, we identify galaxies as satellites of a given host if

(i) their magnitudes fall in the range
$$M_{r,\text{host}} + 1 < M_{r,\text{sat}} < -16,$$

(ii) they are located between 20 kpc and 150 kpc from their host in projected distance (d_{proj}), and

(iii) their velocity offset from the host lies in the range

$$25 \text{ km/s} < |V_{\text{sat}} - V_{\text{host}}| < 300 \text{ km/s} \times e^{-(d_{\text{proj}}/300 \text{ kpc})^{0.8}}.$$

This velocity bound is taken from I14, and is designed to reduce the contamination from interlopers in the satellite sample. Since our interest is in pairs of satellites, we retain only hosts with two or more satellites. Our final sample contains 427 such hosts, with 965 associated satellites. Note that individual hosts are allowed to harbor more than two satellites; on average, the SDSS hosts (as well as our model hosts, see §3) have 2.3 satellites.

2.2 Co-rotation signal

In this subsection, we investigate pairs of satellites for evidence of co-rotation with respect to their host. To facilitate this, we introduce the parameter α, defined as the angle between the line extending from one satellite through the host and the position vector of the second satellite relative to the host, as projected on the sky (see Figure 1). We define this opening angle α such that a satellite pair located on diametrically-opposed sides of a host will have an opening

angle of $0°$. For the duration of this work, we will refer to a satellite pair as "co-rotating" if the satellites have opposite-signed (i.e. one + and one -) line-of-sight velocity offsets relative to their host and their associated opening angle (α) is less than $90°$, or if they have same-signed velocity offsets relative to their host and their associated α is greater than $90°$. Otherwise, the satellite pair is deemed to be counter-rotating.

Figure 2a shows the cumulative number of co-rotating and counter-rotating satellite pairs in our sample as a function of opening angle at $\alpha < 35°$. At small opening angles there is a clear excess of co-rotating pairs, as first reported by I14. The overabundance of co-rotating pairs as a function of α is better illustrated in Figure 2b, which shows the fraction of satellite pairs that are co-rotating as a function of opening angle, computed in distinct bins of α. While the surplus of co-rotating pairs at small opening angle is readily apparent, at $10° < \alpha < 35°$ the signal is consistent with the sample being divided equally between co-rotating and counter-rotating (i.e. a co-rotation fraction of 0.5, as would be expected in the absence of any co-rotating structure). At first glance, the data would seem to indicate the presence of coherently rotating structures that can only be detected at small values of α (i.e. co-rotating planes of satellites viewed close to edge-on).

When examining the co-rotating fraction of satellite pairs over the full range of opening angles (i.e. $0° < \alpha < 180°$), however, the evidence for planes of satellites is far less convincing. In Figure 3, we show (a) the cumulative counts of co-rotating and counter-rotating satellite pairs and (b) the co-rotating fraction, again in discrete bins of α, over the full range of opening angles.[1] In this light, the excess

---

[1] Note that the co-rotating fraction as a function of opening angle

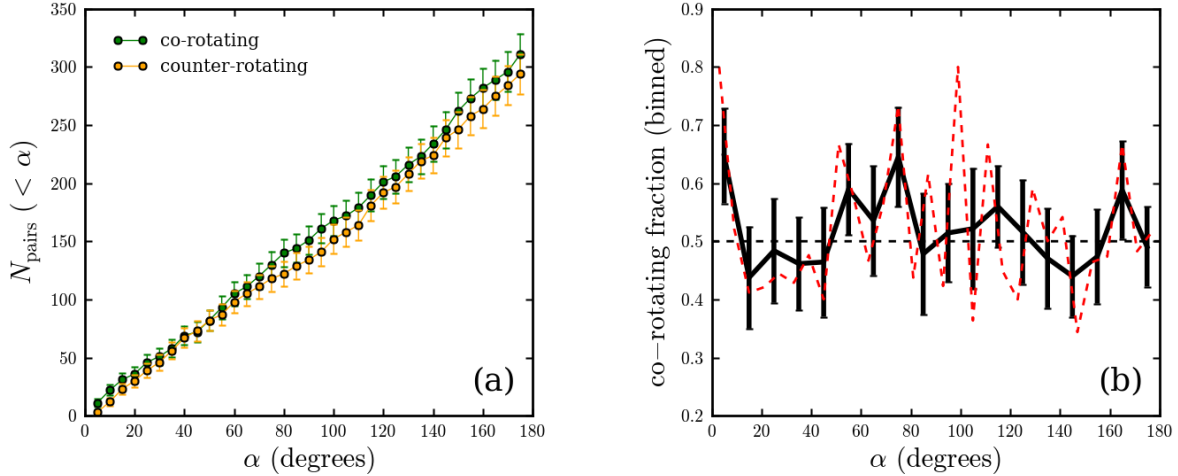**Figure 3.** *Left*: the cumulative number of co-rotating (green line) and counter-rotating (orange line) satellite pairs as a function of α, including Poisson errors, over the full 180° domain. *Right*: the fraction of co-rotating satellite pairs as a function of opening angle, computed in distinct bins of α (bins have width 10°), with error bars derived according to the binomial theorem (solid black line). To facilitate visualization, a coarser binning is adopted than that employed in Fig. 2b; the dash dashed line, however, shows the corresponding dependence of co-rotating fraction on α utilizing this narrower binning. Over the full range of opening angles, the observations are largely consistent with no excess of co-rotating satellite pairs, suggesting an isotropic velocity distribution.

of co-rotating pairs at $\alpha < 10°$ seems less likely to result from structured, coherent rotation associated with planar distributions of satellites. For example, repeatedly resampling 400 satellite pairs placed randomly in phase space (as in our "isotropic" model in §3) will frequently produce satellite samples with excess co-rotating fractions at random opening angles that are, by definition, not indicative of any underlying physics. Thus, care must be taken not to over-interpret the observed overaradundance of co-rotating pairs at small angles, if indeed it is merely the result of random fluctuations associated with undersampling of an underlying isotropic distribution. The remainder of this paper will examine the argument that the excess of co-rotating pairs at small α is significant, and indicative of ubiquitous coherent co-rotation (similar to that observed for M31's satellite population) by comparing the SDSS data to statistical models of satellite kinematics.

3   COMPARISON TO TOY MODELS

In order to gain insight as to whether the data presented in Figures 2 and 3 does indeed argue for the existence of coherently rotating satellite structures, we compare the SDSS data to mock observations of simple, idealized "toy" models of satellite systems. These models are not intended to give

is computed using different binning procedures in Fig. 2b and Fig. 3b, so as to aid in visualization. Our results do not strongly depend on how the data are binned. The increase in co-rotating fraction at small opening angle appears less significant in Fig. 3b as a result of allowing satellite pairs with opening angles of $\sim 10°$ in the innermost bin.

a detailed description of satellite phase-space distributions.[2] However, they do provide a meaningful basis for comparison to the observational data. We begin by detailing how each toy model is constructed:

(i) Isotropic model — For this model, each host is randomly assigned $2 - 5$ satellite galaxies.[3] The position and velocity of each satellite, with respect to the host, is randomly chosen to be between 0 and 200 kpc from the host (with random angular coordinates) and 0 and 200 $km\,s^{-1}$, respectively. The model is randomly rotated and observed along the z direction — i.e. the z direction is taken to be the line-of-sight and the xy plane is taken to be the plane of the sky.

(ii) Disc model — In this model, $2 - 5$ satellites are placed randomly between 0 and 200 kpc from the origin on the xy plane (prior to any rotation taking place) and then randomly given a z coordinate between -10 and 10 kpc. All satellites are assigned a 3D velocity of 100 $km\,s^{-1}$, such that each satellite is in circular motion about the host, initially rotating in the xy plane. The model is then randomly rotated and viewed along the z axis. Finally, to mimic observational error in the line-of-sight velocities, we add to the z component of each satellite's velocity a random offset drawn from a normal distribution with a standard deviation of $\sigma_V = 20$ $km\,s^{-1}$.

---

[2] In particular, the toy models do not account for potential velocity correlations due to group infall, which Cautun et al. (2015) argues may be important, nor do they capture the complexities of observing against a background of interloper galaxies with potentially correllated velocities.

[3] In each case, where the model is permitted to have more than two satellites, we set the probability of a host having n satellites to be four times greater than the probability of having $n + 1$ satellites.

Our qualitative and quantitative results are not strongly dependent upon the assumed velocity structure or thickness of the model satellite discs; since we are only concerned with the sign (+ or -) of the z component (post-rotation) of the satellite's velocity vector, the magnitude of that vector – and any radial dependencies it might have – is largely unimportant.

(iii) M31 model — This model is based on the position and velocities of the 13 satellites belonging to the co-rotating plane identified around M31 by Ibata et al. (2013). The three-dimensional positions of the satellites are taken from McConnachie (2012) and the line-of-sight velocities are compiled from McConnachie (2012) and Collins et al. (2013). Note that we only consider the 13 satellites exhibiting coherent rotation; the two satellites aligned with the planar structure, but with counter-aligned line-of-sight velocities, are excluded. We assign each mock satellite a velocity, such that the radial component of its velocity is consistent with the observed line-of-sight velocities of the true M31 satellites, such that each satellite's total velocity puts it in circular motion around the host.[4] We then randomly select $2-5$ satellites to mock observe (independent of the luminosity of the true M31 satellites), and the system is randomly rotated and viewed along the z axis. We again add to the z component of the velocity a random offset drawn from a normal distribution with $\sigma_V = 30$ km s^{-1}, representative of measurement error in the line-of-sight velocity. While constructed using the positions and velocities of the co-rotating satellites in the M31 plane, it is useful to note that our model is not a true analog of the observed system as every member of the M31 planar structure is fainter (by $\sim 1-2$ magnitudes or more) than our satellite luminosity limit ($M_r < -16$).

(iv) Dumbbell model — In this model, each host is restricted to exactly two satellites. Once the first satellite is randomly placed on the xy plane (again, prior to any rotation), the placement of the second satellite is restricted, such that the opening angle between the two satellites is less than $10°$ when the system is viewed along the z axis. From there, each satellite is assigned a z coordinate between -10 and 10 kpc and the system is subject to random rotation, assigned line-of-sight velocity errors, and finally viewed along the z axis. In essence, this model requires two satellites to be on opposite sides of their hosts and orbiting in rigid-body rotation. As was the case for the disc model, our results do not strongly depend on the adopted thickness of the dumbbell.

For each realization of a model, we rotate the system to a random orientation before observing along the z axis. In our analysis, we simulate a variety of statistical samples, each consisting of $N = 10^6$ model realizations, where most samples include a mix of realizations drawn from the isotropic model along with one of the other three models. For example, the 50% disc + 50% isotropic model consists of 5×10^5 realizations of the disc model and 5×10^5 realizations of the isotropic model. Note that such a sample does *not* consist of 10^6 hosts whose satellites have a 50% probability to be placed in a disc and a 50% probability to be

[4] The origin prior to rotation is taken to be the position of a Milky Way observer.

Model	$p_{\rm sat}$	χ^2	$\tilde{\chi}^2$	p
100% Disc	1.0	460.07	28.76	< 0.001
50% Disc + 50% Isotropic	0.71	179.77	11.39	< 0.001
25% Disc + 75% Isotropic	0.50	71.20	4.45	< 0.001
10% Disc + 90% Isotropic	0.32	22.44	1.40	0.13
50% M31 + 50% Isotropic	0.71	221.79	13.05	< 0.001
50% Dumbbell + 50% Isotropic	0.71	8.70	0.58	0.89
10% Dumbbell + 90% Isotropic	0.32	21.62	1.44	0.12
100% Isotropic	0	11.40	0.67	0.83

Table 1. χ^2, reduced χ^2, and p values based on a comparison of the observed fraction of co-rotating satellite pairs in the SDSS versus that for various statistical samples of model satellite distributions as described in §3. Models in which a large fraction of hosts harbor discs of satellites (including the model based on the M31 plane) are disfavored relative to our dumbbell model or the simple isotropic case. Calculations are made taking satellite pairs over the full range of α (i.e. $0° < \alpha < 180°$), but the p-values are largely unchanged when we restrict the comparison to a narrower range of opening angles (e.g. $\alpha < 35°$). Also shown is the probability that an *individual* satellite is found in a disc traced by bright satellites, $p_{\rm sat}$.

placed randomly. While we do not explicitly explore cases of this type, they are equivalent to the cases we explore that have a percentage disc composition of approximately $p_{\rm sat}^2$, where $p_{\rm sat}$ is the probability of an individual satellite being placed in a disc. Note that this is only an approximation, as some hosts in our models have three or more satellites. For example, a case where satellites of each host independently have a 50% chance of being placed in a disc, would be equivalent to our 25% disc + 75% isotropic model.

In Table 1, we present a summary of our analysis of the χ^2 values describing the goodness of fit for several statistical samples of modeled systems in comparison to the observed fraction of co-rotating satellite pairs as a function of opening angle in the SDSS (see Fig. 3b). The number of degrees of freedom that enter into each p-value calculation is based on how restrictive the model under consideration is: disc models are taken to have one fewer degree of freedom than the purely isotropic model or the model that is based on the observed positions of M31 satellites, since satellites are restricted to being placed in the disc. The dumbbell model essentially introduces an additional constraint on the disc model, so dumbbell models have yet one fewer degree of freedom.

3.1 Disc Model and M31 model

In Figure 4, we show the observed fraction of SDSS satellite pairs that are co-rotating as a function of the opening angle α in comparison to mock observations of various disc models. The thick blue line corresponds to a statistical sample comprised purely of satellite discs, while the green, orange, and magenta lines correspond to samples composed of 50%, 25%, and 10% satellite discs, respectively, with the remainder of each sample consisting of isotropic satellites. In addition, the dashed green line corresponds to a sample with satellites for 50% of the simulated hosts following a M31 model and

the other 50% distributed according to an isotropic satellite population. For comparison, the solid black line shows the co-rotating fraction for a purely isotropic sample.

We find strong disagreement between the fraction of co-rotating satellite pairs as a function of opening angle for models in which 25% or more of hosts harbor planes of satellites in comparison to that for the observed SDSS sample. In particular, the presence of inclined planes (relative to the line-of-sight) in the toy models results in a significant over-abundance of co-rotating pairs at $20° \lesssim \alpha \lesssim 60°$ in comparison to the SDSS observations. Overall, the SDSS data agree reasonably well with models where at most $\sim 10\%$ of hosts have satellites residing in planes (or $\sim 90 - 100\%$ of the hosts have satellites distributed isotropically in phase space); however, the 100% isotropic model does fail to reproduce the overabundance of co-rotating pairs at very small opening angles ($\alpha \lesssim 10°$), as measured in the SDSS sample. As shown in Fig. 4, the M31 sample follows the 50% disc + 50% isotropic sample very closely, as they fundamentally represent the same satellite arrangement (with the caveat that the positions and velocities of the satellites in the M31 model are tailored to match the observed positions of the true M31 satellites). While our results suggest that coherently rotating discs of bright satellites are not common, the objection could be raised that the velocity selection criteria used to select the SDSS systems systematically removes inclined satellite planes (i.e. those systems with satellite pairs at opening angles of $10° \lesssim \alpha \lesssim 170°$); we address this possible selection effect in §3.2.

3.2 Velocity Modeling and Cuts

As highlighted in §3.1, those toy models, in which a high fraction of host galaxies harbor satellite planes, are disfavored in part due to the lack of excess co-rotating satellite pairs at intermediate opening angles (i.e. $20° \lesssim \alpha \lesssim 60°$), corresponding to satellites in discs at non-zero inclination angles. If our sample selection criteria, in particular our velocity cut, are biasing us strongly against such systems, we could perhaps reconcile the apparent discrepancies between the disc models and the SDSS data. In a simplified test case, where each satellite orbits their host in a disc at a velocity of V_0, imposing a velocity cut of exactly V_0 on the host-satellite velocity offset would retain only perfectly edge-on discs, leading to a signal much like the one observed at small opening angles. Relaxing this velocity cut would permit progressively more face-on discs, and imposing no velocity cut would in principle permit any disc inclination angle. In constructing our model, we assigned a characteristic velocity of $100 \, \mathrm{km \, s^{-1}}$ to the satellites and only selected those satellites that have a 1D velocity offset (relative to their host) greater than $\sqrt{2} \times 25 \, \mathrm{km \, s^{-1}}$. Since the toy model is essentially scale-free, this is equivalent to removing satellites that have a 1D velocity offset less than $\sqrt{2} \times 25\%$ of the characteristic 3D velocity for satellites of the host — i.e. a velocity threshold of $0.35 \, V_0$ is applied, where V_0 is the characteristic 3D velocity of the satellites. The higher this velocity cut, the more we would expect a contribution to the co-rotating fraction at intermediate α from inclined discs to be suppressed, as such systems would have a significant component of their velocity moving perpendicular to the line-of-sight.

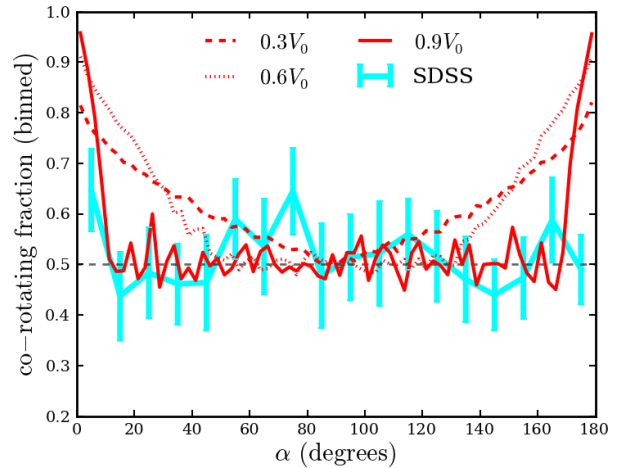In Figure 5, we demonstrate the impact of altering our

Figure 5. The fraction of co-rotating satellite pairs in the SDSS satellite sample (cyan line) and in the 25% disc + 75% isotropic model (red lines), varying the value of the velocity selection limit applied to the models. The dotted, dashed, and solid red lines correspond to models in which only systems with $\Delta V_{los} > 0.3$, 0.6, 0.9 V_0 are included, respectively, and where V_0 denotes the 3D characteristic velocity of satellites in the plane/disc. The dramatic overabundance of co-rotating pairs at small α in the SDSS data is only captured by models that contain nearly exclusively edge-on discs (i.e. applying the $\Delta V_{los} > 0.9 \, V_0$ cut).

velocity selection criterion on the measured co-rotation fraction versus opening angle for the 10% disc + 90% isotropic model. The various red lines range from selection limits of 30% of the 3D velocity to 90% of the 3D velocity, with the SDSS data included for comparison (cyan line). Reproducing the lack of excess co-rotation at $20° \lesssim \alpha \lesssim 60°$ — or similarly the sharpness of the increase in co-rotating satellite pairs at very small α — requires a very high velocity cut (i.e. $\sim 0.9 V_0$). Given that our adopted velocity limit is $\Delta V_{los} > \sqrt{2} \times 25 \, \mathrm{km \, s^{-1}}$, such a strong selection bias would require that the characteristic velocity (V_0) of satellites in planes would need to be $\sim 40 \, \mathrm{km \, s^{-1}}$. If the planar satellites have such low velocities, a velocity cut of $\sqrt{2} \times 25 \, \mathrm{km \, s^{-1}}$ would indeed correspond to 0.9 times the characteristic velocity of the plane members, and we could confidently state that we had removed all but edge-on planes.

The "toy model" adopted by I14 as a comparison to their measurements of the co-rotating satellite fraction in the SDSS utilizes exactly this characteristic velocity ($40 \, \mathrm{km \, s^{-1}}$); as a result, their toy model only includes edge-on (or nearly edge-one) discs, thereby reproducing the overabundance of co-rotating satellite pairs at small opening angles (see their Fig. 1b). Assuming a 3D characteristic velocity of $40 \, \mathrm{km \, s^{-1}}$ for satellites in planes, however, is inconsistent with the broad expectations from subhalo kinematics in N-body simulations as well as the observed line-of-sight velocities of satellites in the M31 plane, which have a median value of $|\Delta V_{los}| \sim 92 \, \mathrm{km \, s^{-1}}$. Moreover, such a low characteristic velocity directly conflicts with the measured line-of-sight velocity offsets of the co-rotating satellite pairs identified by I14 (see their Table 1) as well as those in our sample.

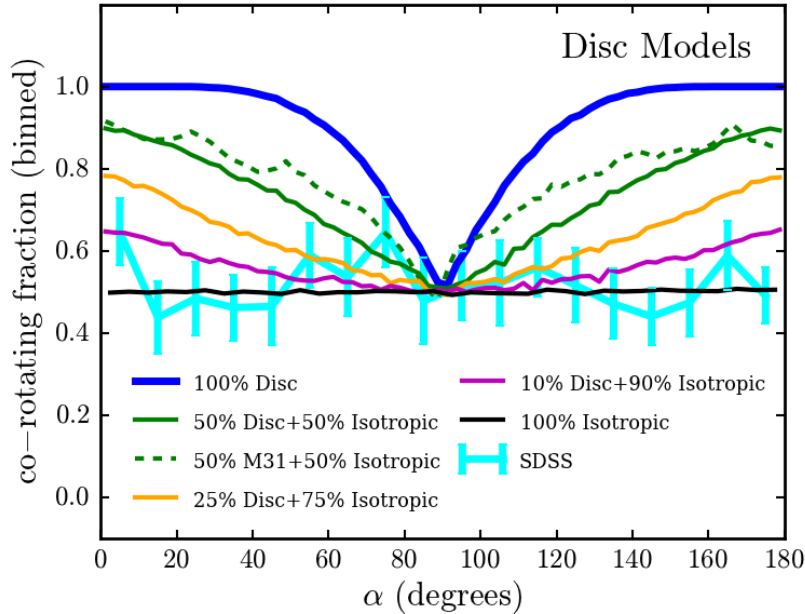Figure 6 shows the host-satellite (line-of-sight) veloc-

Figure 4. The fraction of co-rotating satellite pairs as a function of opening angle (α) for various versions of the disc model, including the model based on the M31 plane, in comparison to the observed co-rotating fraction measured in the SDSS (cyan line). The observed kinematics of bright satellites in the SDSS are consistent with at most 10% of hosts having disc-like or planar satellite distributions, with the remainder being distributed isotropically.
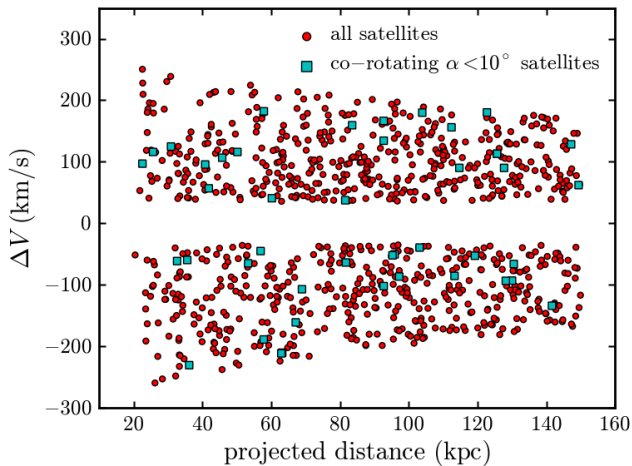

Figure 6. The line-of-sight velocity offset for each satellite in the SDSS sample relative to its host as a function of its projected distance from the host (red circles). Those satellites corresponding to co-rotating pairs with opening angles of $\alpha < 10°$ are highlighted as cyan squares. Given that most satellites in the sample (especially those that are co-rotating and at small opening angles) have velocity offsets greater than the lower selection limit, we conclude that our observational sample is not strongly biased against inclined planes (or discs).

ity offset plotted against host-satellite projected distance for each satellite in our SDSS sample, highlighting those systems belonging to pairs with $\alpha < 10°$. The mean absolute value of the 1D (line-of-sight) velocities for the 44 satellites in co-rotating pairs with $\alpha < 10°$ is $109.4 \ \mathrm{km \, s^{-1}}$, consistent with that for the overall sample ($111.4 \ \mathrm{km \, s^{-1}}$).

This indicates that a velocity cut of $\sqrt{2} \times 25 \ \mathrm{km \, s^{-1}}$ would be insufficient to select only edge-on planes, such that we should also detect co-rotation from planes at moderate inclination angles (i.e. yielding an elevated co-rotating fraction at $10° < \alpha < 60°$). As a result, we argue that the observational data are inconsistent with co-rotating planes being ubiquitous in the local Universe — at least with respect to satellites brighter than $M_r = -16$.

3.3 Dumbbell model

Recognizing that the observed variation in co-rotating satellite fraction with opening angle is strongly inconsistent with discs or planes of satellites being prevalent, we now discuss a potential alternative scenario: the dumbbell model (see §3). Figure 7 shows the co-rotating satellite fraction as a function of opening angle for the SDSS satellite sample in comparison to two formulations of the dumbbell model, one with 50% dumbbells (and 50% isotropic satellites) and one with 10% dumbbells (and 90% isotropic satellites). Both models are in relatively good agreement with the observational data. In particular, the dumbbell model is able to reproduce the observed overabundance of co-rotating pairs at small opening angles and the corresponding sharp decrease at $\alpha \sim 10°$. In §4, we address the physical motivation (or lack thereof) for dumbbell-like satellite configurations. For now, we note that the dumbbell model yields a better fit to the observed kinematic data than the disc model. The p-value for the toy model with 10% contribution from dumbbells is 0.948, meaning we fail to reject it at any confidence level. We also fail, at the 90% confidence level, to reject the 50% dumbbell model ($p = 0.152$). While we similarly fail to reject the 10%
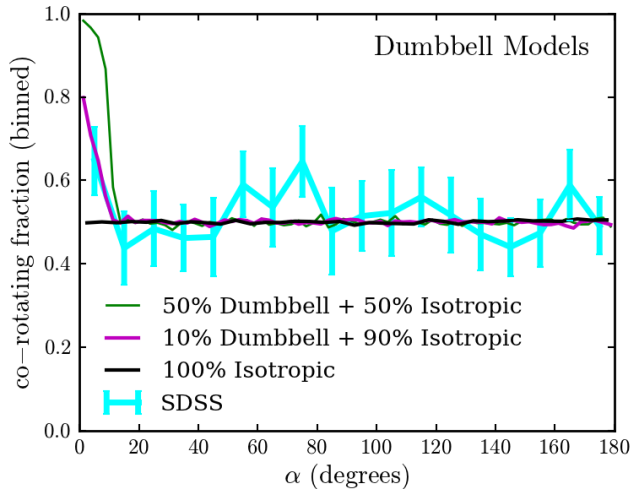
Figure 7. The fraction co-rotating satellite pairs as a function of opening angle α for the observed SDSS sample (cyan line) and various simulated dumbbell samples (green, magenta, and black lines). While unlikely to be physically accurate, a model in which a small fraction ($\sim 10\%$) of massive galaxies host satellites in dumbbell-like distributions is able to reproduce the overabundance of co-rotating satellites pairs at small opening angles.

disc model at 90% confidence ($p = 0.223$), we reject all other disc models at $> 99\%$ confidence (see Table 3).

4   DISCUSSION

Our analysis is motivated by the work of I14, which found an increase in the incidence of co-rotation in satellite pairs very near diametric opposition with respect to their host. If this excess co-rotation is the result of physical processes, it would tell us something significant about the co-evolution of satellite systems and the behavior of dark matter on small scales – perhaps indicating a serious problem with the ΛCDM model. On the other hand, we must consider the possibility that the co-rotation signal of I14 is not robust and is the product of random chance. In this section, we weight these competing possibilities.

In selecting our sample, we adhere closely to the selection criteria of I14; however, we did not reproduce the I14 satellite sample exactly. Of the host systems listed in Table 1 of I14, two galaxies fail our selection criteria. In one of these cases, the host magnitude fell just outside of our selection window, while the other host had a neighbor of nearly equal, but slightly brighter magnitude ($\Delta M_r = 0.01$). In addition, our selection includes several systems not identified by I14, though we do not expect these differences between our samples to bias our results in any meaningful way. Of the 22 satellite pairs with $\alpha < 8°$ in I14, 20 (91%) appear in our sample. Moreover, we reproduce the principal result from I14, finding an excess of co-rotating satellite pairs located on diametrically-opposed sides of their host galaxy (i.e. at small opening angles). At $\alpha < 8°$, we find 21 out of 27 satellite pairs to be co-rotating, corresponding to a co-rotating fraction of $0.78 \pm 0.08\%$.

However, when examining the kinematics of the entire population of satellite pairs (i.e. at all opening angles), the

dependence of co-rotating fraction on α is inconsistent with the expectations from simple models of rotating discs (or planes) of satellites. For example, at large α, we would naively expect an overabundance of co-rotating satellites mirroring that detected at small opening angles. Ibata et al. (2014b) argue that caution must be taken when considering satellites on the same side of the host, as relative motion of the satellites with respect to each other (e.g. in orbital binary pairs) could dominate the motion of a satellite around the host, particularly when viewed in projection. As a result, when examining satellite pairs with large opening angles, Ibata et al. (2014b) require that the brighter of the satellite pair be at least two magnitudes fainter than the host to minimize the impact of infalling sub-groups; to mitigate deblending problems, identified pairs closer than 25 kpc in separation are also excluded. With these cuts in place, the I14 sample contains 15 pairs of satellites with $\alpha > 172°$, 10 of which are co-rotating (Ibata et al. 2014b). Applying identical cuts to our sample, we find 13 out of 21 satellites co-rotating over the same range in α, while removing these additional selection criteria yields 44 pairs of satellites, 23 of which are co-rotating. In each case, the satellite sample at large α is divided nearly evenly between co-rotating and counter-rotating pairs, and the co-rotating excess at large α is significantly less substantive than that at small α. This agrees well with the work of Cautun et al. (2015), which also finds no evidence of excess co-rotation in satellite pairs located on the same side of their host.

The differences between the expected kinematics of satellites belonging to discs (or planes) and that observed in the SDSS satellite sample extend far beyond the large α regime. If the observed overabundance of co-rotating satellite pairs at small α is associated with a large population of satellite planes, then we would expect that planes at non-zero inclination angles to contribute co-rotating pairs at intermediate opening angles to the observed sample, resulting in a gradual decrease in the co-rotating fraction at $0° < \alpha < 90°$ (see Fig. 4). Instead, what is observed is a precipitous drop in the co-rotating fraction, with 21 out of 27 ($78 \pm 8.0\%$) satellite pairs found to be co-rotating at $\alpha < 8°$, but only 27 out of 63 pairs ($44 \pm 6.2\%$) co-rotating over $8° < \alpha < 28°$. Moreover, the dependence of co-rotating fraction on α is quite noisy (see Fig. 3), such that excesses in the co-rotating fraction – comparable to that found at $\alpha < 10°$ – are detected at other relatively narrow ranges of opening angle. For example, 20 out of the 31 satellite pairs with $70° < \alpha < 80°$ are co-rotating, which (if significant) is difficult to reconcile with the predicted kinematics of satellites in planes. The discrepancies between the data and the disc models are borne out in the statistical analysis, with models involving more than 10% contribution from discs (or planes) strongly disfavored (see Table 1). This is in good agreement with the predictions of Cautun et al. (2015), which argue that only $\sim 15\%$ of bright satellites should share a coherent sense of rotation to within $25°$, as would be required for planar co-rotation. Our analysis strongly disfavors the claim that planar configurations of satellites are ubiquitous over the magnitude range ($M_r < -16$) considered.

While the disc model does a relatively poor job of replicating the observational data, our toy model with satellites arranged in dumbbell configurations provides a better fit to the observed satellite kinematics. By construction, the satel-

lites in the dumbbell model are located at opposition, such that they able to replicate the sharpness of the increase in co-rotating fraction at small α while being consistent with no excess co-rotation at larger opening angles. The physicality of the dumbbell model is questionable, however, as it is difficult to imagine a scenario that involves satellites co-rotating in such a highly-constrained configuration. Additionally, the satellites belonging to M31's plane are not in a dumbbell configuration. For these reason, we conclude that the data are not likely to be the result of dumbbell configurations either.

In the absence of viable alternative models, we argue that the excess of co-rotating satellite pairs at small α is very likely the result of random noise. Among the disc models, only the model with a 10% contribution from satellite discs is a comparably good fit to the SDSS data as the purely isotropic model. Moreover, 25% of random realizations of an isotropic model comprised of 400 hosts (i.e. comparable in number to the observed SDSS sample) yield excess co- and counter-rotating pairs of satellites comparable in significance to that measured in the SDSS sample, although just $\sim 1-2\%$ show an overabundance of co-rotating pairs at small opening angles ($\alpha < 20°$).

These results should not be taken to say that there are no planes of satellites in the Universe. Statistically, the observational data are roughly consistent with $\lesssim 10\%$ of isolated, massive galaxies playing host to planes, or more specifically planes with multiple luminous satellites. Our result does not exclude the possibility that planar structures preferentially populated by faint satellites could be ubiquitous; if true, this could provide powerful insight into the formation of planar satellite structures. With the caveat that all of the satellites under our consideration here are brighter than the satellites belonging to the M31 plane, we exclude the possibility of ubiquitous planes analogous to the M31 plane at a very high confidence level.

5 CONCLUSIONS

In this work, we investigate the ubiquity of co-rotating planes of satellites similar to that observed around M31. Using data drawn from the SDSS, we study the orientation and kinematics of bright ($M_r < -16$) satellite pairs around isolated galaxies, selected to be roughly analogous to the Milky Way and M31. By comparing the fraction of co-rotating satellites pairs as a function of opening angle to the predictions of simple models, we investigate the signatures of coherent rotation arising from satellites arranged in planar structures. Our findings are as follows:

- We confirm an excess of co-rotating pairs of satellites at opening angles of $\alpha < 10°$ — i.e. satellite pairs located on diametrically-opposed sides of their host (see Fig. 2). This overabundance of co-rotating pairs at small opening angles, as first identified by I14, has been cited as evidence that 50% of satellites belong to coherently-rotating planes (Ibata et al. 2014b).

- We find that the excess of co-rotating pairs at small opening angles is unlikely to be due to ubiquitous co-rotating planes of satellites. While the behavior at small α is suggestive of planes aligned along the line-of-sight (i.e. with an orbital inclination of zero), the signal is strongly inconsistent with mock observations of satellite galaxy planes (or discs). In particular, we find no contribution to the co-rotating fraction from planes inclined relative to the line-of-sight (i.e. with satellites configured at opening angles of $10° \lesssim \alpha \lesssim 60°$). For our sample of isolated systems, we find that at most $\sim 10\%$ of hosts harbor satellites planes – as traced by the luminous (LMC-like) satellite population.

- The excess of co-rotating pairs of satellites at small α is better fit by a "dumbbell" model, where satellites have co-rotating partners located opposite the host galaxy (but not a true plane). However, this model is very likely unphysical.

- We do not rule out the possibility that $\sim 10\%$ of hosts having co-rotating planes of satellites, or correspondingly $\sim 30\%$ of satellites residing in such planes. This case is similar enough to the isotropic case that the observed SDSS co-rotating fraction as a function of opening angle is roughly consistent with $\lesssim 10\%$ of massive host galaxies harboring planes of satellites.

REFERENCES

Abazajian K. N. et al., 2009, ApJS, 182, 543

Astropy Collaboration et al., 2013, A&A, 558, A33

Azzaro M., Patiri S. G., Prada F., Zentner A. R., 2007, MNRAS, 376, L43

Bailin J. et al., 2005, ApJ, 627, L17

Bailin J., Power C., Norberg P., Zaritsky D., Gibson B. K., 2008, MNRAS, 390, 1133

Blanton M. R., Roweis S., 2007, AJ, 133, 734

Blanton M. R. et al., 2005, AJ, 129, 2562

Blumenthal G. R., Faber S. M., Primack J. R., Rees M. J., 1984, Nature, 311, 517

Brainerd T. G., 2005, ApJ, 628, L101

Buck T., Macci'o A. V., Dutton A. A., 2015, ArXiv e-prints

Cautun M., Bose S., Frenk C. S., Guo Q., Han J., Hellwing W. A., Sawala T., Wang W., 2015, ArXiv e-prints

Cautun M., Wang W., Frenk C. S., Sawala T., 2015, MNRAS, 449, 2576

Collins M. L. M. et al., 2013, ApJ, 768, 172

Conn A. R. et al., 2013, ApJ, 766, 120

Davis M., Efstathiou G., Frenk C. S., White S. D. M., 1985, ApJ, 292, 371

Deason A. J. et al., 2011, MNRAS, 415, 2607

Faltenbacher A., Li C., Mao S., van den Bosch F. C., Yang X., Jing Y. P., Pasquali A., Mo H. J., 2007, ApJ, 662, L71

Hao J., Kubo J. M., Feldmann R., Annis J., Johnston D. E., Lin H., McKay T. A., 2011, ApJ, 740, 39

Holmberg E., 1969, Arkiv for Astronomi, 5, 305

Ibata N. G., Ibata R. A., Famaey B., Lewis G. F., 2014a, Nature, 511, 563

Ibata R. A., Famaey B., Lewis G. F., Ibata N. G., Martin N., 2014b, ArXiv e-prints

Ibata R. A., Ibata N. G., Lewis G. F., Martin N. F., Conn A., Elahi P., Arias V., Fernando N., 2014c, ApJ, 784, L6

Ibata R. A. et al., 2013, Nature, 493, 62

Kang X., van den Bosch F. C., Yang X., Mao S., Mo H. J., Li C., Jing Y. P., 2007, MNRAS, 378, 1531

Karachentsev I., 1996, A&A, 305, 33

Knebe A., Gill S. P. D., Gibson B. K., Lewis G. F., Ibata R. A., Dopita M. A., 2004, ApJ, 603, 7

Koch A., Grebel E. K., 2006, AJ, 131, 1405

Komatsu E. et al., 2011, ApJS, 192, 18

Kroupa P. et al., 2010, A&A, 523, A32

Kroupa P., Theis C., Boily C. M., 2005, A&A, 431, 517

Kunkel W. E., Demers S., 1976, in Royal Greenwich Observatory Bulletins, Vol. 182, The Galaxy and the Local Group, Dickens R. J., Perry J. E., Smith F. G., King I. R., eds., p. 241

Libeskind N. I., Cole S., Frenk C. S., Okamoto T., Jenkins A., 2007, MNRAS, 374, 16

Libeskind N. I., Frenk C. S., Cole S., Helly J. C., Jenkins A., Navarro J. F., Power C., 2005, MNRAS, 363, 146

Libeskind N. I., Hoffman Y., Tully R. B., Courtois H. M., Pomarede D., Gottloeber S., Steinmetz M., 2015, ArXiv e-prints

Libeskind N. I., Knebe A., Hoffman Y., Gottlöber S., Yepes G., Steinmetz M., 2011, MNRAS, 411, 1525

Lovell M. R., Eke V. R., Frenk C. S., Jenkins A., 2011, MNRAS, 413, 3013

Lynden-Bell D., 1976, MNRAS, 174, 695

McConnachie A. W., 2012, AJ, 144, 4

McConnachie A. W., Irwin M. J., 2006, MNRAS, 365, 902

Metz M., Kroupa P., Jerjen H., 2007, MNRAS, 374, 1125

Metz M., Kroupa P., Jerjen H., 2009, MNRAS, 394, 2223

Metz M., Kroupa P., Libeskind N. I., 2008, ApJ, 680, 287

Moore B., Governato F., Quinn T., Stadel J., Lake G., 1998, ApJ, 499, L5

Pawlowski M. S. et al., 2014, MNRAS, 442, 2362

Pawlowski M. S., Kroupa P., 2013, MNRAS, 435, 2116

Pawlowski M. S., Kroupa P., Angus G., de Boer K. S., Famaey B., Hensler G., 2012, MNRAS, 424, 80

Pawlowski M. S., Kroupa P., Jerjen H., 2013, MNRAS, 435, 1928

Pawlowski M. S., McGaugh S. S., 2014, ApJ, 789, L24

Pawlowski M. S., Pflamm-Altenburg J., Kroupa P., 2012, MNRAS, 423, 1109

Peñarrubia J., Kroupa P., Boily C. M., 2002, MNRAS, 333, 779

Plionis M., Benoist C., Maurogordato S., Ferrari C., Basilakos S., 2003, ApJ, 594, 144

Sales L., Lambas D. G., 2004, MNRAS, 348, 1236

Sales L., Lambas D. G., 2009, MNRAS, 395, 1184

Tempel E., Guo Q., Kipper R., Libeskind N. I., 2015, ArXiv e-prints

Tully R. B., Libeskind N. I., Karachentsev I. D., Karachentseva V. E., Rizzi L., Shaya E. J., 2015, ArXiv e-prints

van den Bosch F. C., Lewis G. F., Lake G., Stadel J., 1999, ApJ, 515, 50

Wang J., Frenk C. S., Cooper A. P., 2013, MNRAS, 429, 1502

West M. J., Blakeslee J. P., 2000, ApJ, 543, L27

White S. D. M., Rees M. J., 1978, MNRAS, 183, 341

Yang X., van den Bosch F. C., Mo H. J., Mao S., Kang X., Weinmann S. M., Guo Y., Jing Y. P., 2006, MNRAS, 369, 1293

York D. G. et al., 2000, AJ, 120, 1579

Zaritsky D., Gonzalez A. H., 1999, PASP, 111, 1508

Zaritsky D., Smith R., Frenk C. S., White S. D. M., 1997, ApJ, 478, L53

Zentner A. R., Kravtsov A. V., Gnedin O. Y., Klypin A. A., 2005, ApJ, 629, 219